Pseudogene CSPG4P12 affects the biological behavior of non-small cell lung cancer by Bcl-2/Bax mitochondrial apoptosis pathway

WENQIAN HU[1,2], HONGJIAO WU[1], ANG LI[1], XUAN ZHENG[1],
WENLI ZHANG[3], QINQIN TIAN[2] and XUEMEI ZHANG[1,2]

[1]School of Public Health, [2]College of Life Sciences and [3]Comprehensive Testing and Analytical Center,
North China University of Science and Technology, Tangshan, Hebei 063210, P.R. China

Abstract. Increasing evidence has shown that chondroitin sulfate proteoglycan 4 (CSPG4) serve a critical role in tumor progression. However, the roles of chondroitin sulfate proteoglycan 4 pseudogene 12 (CSPG4P12) remain to be elucidated. The present study aimed to investigate the potential effects of CSPG4P12 on the physiological behaviors of non-small cell lung cancer (NSCLC) and its underlying biological mechanism. The expression levels of CSPG4P12 in NSCLC tissues and adjacent normal tissues were analyzed using the gene expression profiling interactive analysis 2 database and reverse transcription-quantitative PCR. Cell Counting Kit-8 and colony formation assays were performed to measure cell proliferation. In addition, Transwell and wound healing assays were performed to assess cell invasion and migration. Cell adhesion was measured by cell-extracellular matrix adhesion assay. Hoechst 33342 staining assay was performed to detect nucleoli of apoptotic cells, and transmission electron microscopy (TEM) was utilized for apoptosis detection. Immunofluorescence and western blot assays were performed to measure the expression levels of apoptosis-related proteins. The present results revealed that the expression levels of CSPG4P12 in NSCLC tissues were significantly lower compared with those in adjacent normal tissues. Overexpression of CSPG4P12 inhibited cell proliferation, invasion, migration and adhesion whilst promoting apoptosis. There were missing mitochondrial cristae and mitochondrial vacuoles in the CSPG4P12-overexpressed cells when observed under TEM. Overexpression of CSPG4P12 also increased the expression of Bax and p53, whereas it inhibited the expression of Bcl2. In conclusion, CSPG4P12 could inhibit NSCLC development and tumorigenesis by activating the p53/Bcl2/Bax mitochondrial apoptotic pathway.

Introduction

Lung cancer is one of the most prevalent malignant tumors and seriously threatens human health, since it can drastically reduce the quality of life (1). The latest statistics show that there are about 19.3 million new lung cancer cases and nearly 10 million mortalities worldwide (2). Non-small cell lung cancer (NSCLC) is the most common pathological subtype (~80%) of lung cancer globally (3). Despite the availability of various treatment options for NSCLC, such as surgery, chemotherapy, nanomedicines, photodynamic therapy and immune checkpoint inhibitors, its mortality rate remains high (4-6). It is therefore important to uncover the mechanism that can mediate the process of NSCLC development. The occurrence and progression of NSCLC have been reported to be influenced by genetic factors and various environmental factors, such as smoking, air pollution and occupational exposure (7).

Previous studies have suggested that pseudogenes serve an important role in the development of cancer (8,9). Pseudogenes typically arise from mutations or inactivation of genes, which accumulate during the evolution process (10). Initially, they were dismissed as non-functional genomic junk (11). However, recent studies have revealed that dysregulated pseudogenes, such as double homeobox a pseudogene 8 (DUXAP8) and cathepsin l pseudogene 8 (CTSLP8) can affect oncogenic progression by regulating that of particular cancer-related genes (12,13). In particular, pseudogene-derived long non-coding RNAs (lncRNAs), such as DUXAP8 and KRT17P3 (keratin 17 pseudogene 3), which can function as either oncogenes or tumor suppressors, have been previously implicated in cell proliferation, migration and invasion, in addition to drug resistance in NSCLC (12,14). However, the underlying molecular mechanisms of a large number of pseudogenes remain unclear.

Correspondence to: Dr Xuemei Zhang, College of Life Sciences, North China University of Science and Technology, 21 Bohai Road, Caofeidian Xincheng, Tangshan, Hebei 063210, P.R. China
E-mail: jyxuemei@gmail.com

Chondroitin sulfate proteoglycan 4 (CSPG4) pseudogene 12 (CSPG4P12) is a pseudogene-derived lncRNA that is highly homologous with its parent gene CSPG4 (15). CSPG4 has been reported to serve an important role in the occurrence and development of various types of cancer, such as anaplastic thyroid cancer, squamous cell carcinoma of head and neck and basal breast carcinoma (16,17). Functionally, CSPG4 is a tumor cell surface cancer antigen that can confer phenotypic heterogeneity and mediate malignant progression in epithelial ovarian cancer (18). It has also been previously revealed that the overexpression of CSPG4 in anaplastic thyroid cancer (ATC) can increase tumor size of ATC patient-derived xenografted mice (17). In addition, a number of studies have identified pseudogenes, such as PTENP1 (phosphatase and tensin homolog pseudogene 1) and AGPG (actin gamma 1 pseudogene), to be important components of gene regulation networks (19,20). Therefore, present study hypothesized that CSPG4P12 may be involved in the occurrence and progression of NSCLC.

In the present study, after analyzing the differences of the expression of CSPG4P12 between NSCLC tissues and adjacent normal tissues, the effect of CSPG4P12 on the physiological behaviors of NSCLC was evaluated to assess its potential mechanism.

Materials and methods

Tissue specimens. A total of 19 NSCLC tissues and corresponding adjacent healthy tissues were obtained from Tangshan Gongren Hospital Affiliated to North China University of Science and Technology (NCST; Tangshan, China) from March 2021 to July 2021. All subjects (age range, 43-81 years; median age, 63 years; 11 males and 8 females) were included with postoperative pathological diagnosis of NSCLC and individuals who had received any preoperative treatment were excluded. The present study was approved by the Ethics Committee of NCST (approval no. 2021036) and all participants or their family members signed informed consent forms.

Differential expression analysis. Gene expression profiling interactive analysis 2 database (http://gepia2.cancer-pku.cn/#analysis) was utilized to perform the differential expression analysis of CSPG4P12 between cancer tissues and adjacent normal tissues in NSCLC (21). Based on datasets from The Cancer Genome Atlas and genotype-tissue expression project, 483 lung adenocarcinoma and 347 healthy tissues, 486 lung squamous cell carcinoma tissues and 338 healthy tissues were involved in the present study using a standard processing pipeline. The key search terms used were as follows: 'CSPG4P12' in the search box on the home page, then 'Boxplots'; other parameters were the initial value and the 'LUAD' and 'LUSC' data sets were selected.

Cell culture and plasmid transfection. NSCLC A549 and H1299 cell lines (Procell Life Science & Technology Co., Ltd.) were cultured in RPMI 1640 medium (Thermo Fisher Scientific, Inc.) supplemented with 10% FBS (Zhejiang Tianhang Biotechnology Co., Ltd.) at 37℃ with 5% CO_2. The CSPG4P12-pUC57 plasmid was constructed by Changzhou Ruibo Bio-Technology Co., Ltd.

In brief, CSPG4P12 (ENST00000558282.5; CSPG4P12-201; 4,853 bp) was amplified using KOD FX (cat. no. KFX-101; Toyobo Life Science) and the following primers (SinoGenoMax Co., Ltd.): 5'-CTAGTCTAGACACCTGGGCACCAACCTC-3' (*Xba*I) and 5'-ACGCGTCGACATAGAAAACAGCCCCAACCAG-3' (*Sal*I). The thermocycling conditions were: Pre-denaturation at 95℃ for 3 min; followed by 25 cycles at 95℃ for 25 sec, at 60℃ for 20 sec and 72℃ for 40 sec; final extension at 72℃ for 1 min. The PCR product was recombined into the pUC57 vector (429-452 nt) to generate the CSPG4P12 overexpression plasmid (CSPG4P12-pUC57), which was verified by Sanger sequencing.

Cells were seeded into six-well plates with a density of $1x10^6$ cells/well. Cells were transfected at ~80% confluency with 2.5 μg CSPG4P12-pUC57 or empty plasmid (pUC57) using Lipofectamine® 2000 (Thermo Fisher Scientific, Inc.) at 37℃ for 5 h according to the manufacturer's protocols. Cells were then harvested for further analysis after 24 h. Cells were transfected with (negative control) or without (blank control) 2.5 μg pUC57 plasmid for detected the effects of pUC57 plasmid on the proliferation of NSCLC cells.

Reverse transcription-quantitative PCR (RT-qPCR). Total RNA was extracted using the TRIzol® reagent (Invitrogen; Thermo Fisher Scientific, Inc.). According to the manufacturer's instructions, cDNA was synthesized from 2 μg total RNA using RevertAid First Strand cDNA Synthesis kit (cat. no. K1622; Thermo Fisher Scientific, Inc.). 20 ng of cDNA was then used for qPCR with the Power SYBR-Green PCR Master Mix (cat. no. A25742; Thermo Fisher Scientific, Inc.) via a 7900HT Fast Real-Time PCR System (Thermo Fisher Scientific, Inc.) with GAPDH as the internal reference. The following primer pairs, which were obtained from SinoGenoMax Co., Ltd., were used for qPCR: CSPG4P12 forward, 5'-ATGGACCAGTACCCCACACG-3' and reverse, 5'-CCCTGCCTCTAGCCATTGAC-3' and GAPDH forward, 5'-CTGGGCTACACTGAGGACC-3' and reverse, 5'-AAGTGGTCGTTGAGGGCAATG-3'. The thermocycling conditions were as follows: Pre-denaturation at 95℃ for 2 min; followed by 40 cycles at 95℃ for 15 sec and at 59℃ for 1 min; final extension at 72℃ for 10 min. The relative expression levels of CSPG4P12 were calculated using the $2^{-\Delta\Delta Cq}$ method (22).

Cell proliferation assay. CCK-8 assay was performed to detect cell viability. A total of $5x10^3$ transfected cells/well were seeded into a 96-well plate. After culturing for 24, 48 and 72 h at 37℃, cells were mixed with 10 μl CCK-8 reagent (Dojindo Molecular Technologies, Inc.) for 2 h at 37℃. The absorbance at 450 nm was measured using the Infinite M200 PRO Microplate Reader (Tecan Group, Ltd.).

Colony formation assay. For the colony formation assay, transfected A549 or H1299 cells were seeded into 60-mm dishes at a density of $2x10^3$ cells/dish and allowed to grow in RPMI 1640 medium supplemented with 10% FBS at 37℃ for 10 days, then fixed with 4% polyformaldehyde at 37℃ for 30 min and stained with 0.1% crystal violet (Beijing Solarbio Science & Technology Co., Ltd.) at 37℃ for 10 min. A light microscope (magnification, x40; Olympus Corporation) was used for observation. Each colony contained >50 cells, ranging

in size from 0.3-1.0 mm. The colonies were detected using ImageJ (v1.42q; National Institutes of Health).

Cell migration and invasion. Transwell assay was performed to measure cell migration and invasion. A total of 7×10^4 plasmid-transfected cells in RPMI1640 medium were seeded into the upper chambers (6.5-mm diameter inserts; 8-μm pore size; Costar; cat. no. 3422; Corning, Inc.) with or without 50 mg/l Matrigel precoating (Corning, Inc.) at 37˚C for 5 h. The lower chamber was filled with RPMI1640 medium supplemented with 20% FBS. Cells attached in the upper chamber were then removed after 24 (for migration assay) or 48 h (for invasion assay) at 37˚C. The chambers were fixed with 4% paraformaldehyde for 30 min at 37˚C and then stained with 0.1% crystal violet at 37˚C for 10 min. Migrating or invading cells were then observed and imaged under an inverted light microscope (magnification, x100; Olympus Corporation). A total of five fields (upper, lower, left, right, and middle) were selected per chamber for quantification.

Wound healing and adhesion assay. Untransfected A549 or H1299 Cells were seeded into a six-well plate at a density of 1×10^6 cells/well and cultured in RPMI1640 medium supplemented with 1% FBS until ~80% confluency. The cell monolayer was then scraped in a straight line to create a 'scratch' with a 200 μl pipette tip. Images were captured under an inverted light microscope (magnification, x40) after 0, 24 and 48 h incubation at 37˚C. The width of wound was detected using ImageJ (v1.42q; National Institutes of Health). To measure cell adhesion, a 96-well plate was coated with 50 mg/l Matrigel at 37˚C for 5 h, then blocked with 1% bovine serum albumin (Thermo Fisher Scientific, Inc.) at 37˚C for 2 h. Transfected cells were then seeded at the density of 2×10^4 cells/well. The images under an inverted light microscope (x100; Olympus Corporation) were captured at 30, 60 and 90 min timepoints at 37˚C. CCK-8 assay was utilized to detect the cell proliferation on a microplate reader as aforementioned.

Hoechst 33342 staining assay. Transfected cells were cultured for 48 h at 37˚C, fixed with 4% polyformaldehyde for 30 min at 37˚C, washed with PBS and then stained with 1 μg/ml Hoechst33342 (Beijing Solarbio Science & Technology Co., Ltd.) in the dark for 20 min at 37˚C. Nuclear condensation and fragmented nuclei was observed under a fluorescent inverted microscope (magnification, x100; Olympus Corporation).

Transmission electron microscopy (TEM). Cells were collected after transfection, and centrifuged at 1,000 x g for 10 min at 37˚C to form a pellet. Cell pellets were fixed with 2.5% glutaraldehyde at 4˚C overnight and then washed three times with 0.1 M PBS (pH 7.4) for 15 min. The 1% osmium tetroxide was fixed again at room temperature for 2 h in the dark and then washed 15 min for three times with 0.1M PBS (pH 7.4). A gradient dehydration was performed using ascending concentrations of ethanol. The samples were embedded with the 812 resin embedding medium (Beijing Zhongjingkeyi Technology Co., Ltd.) overnight at 37˚C and subsequently polymerized at 60˚C for 12 h. The embedded

samples were cut into 60-nm ultra-thin sections using a microtome (EM UC6; Leica Microsystems, Inc.). Finally, the sections were double-stained with 3% lead citrate and 1.5% uranyl acetate at 37˚C for 20 min. Observation and acquisition of images were performed by TEM (x10,000; H-7650; Hitachi, Ltd.).

Immunofluorescence (IF) assay. Untransfected A549 or H1299 Cells were seeded into a six-well plate at a density of 5×10^5 cells/well. After 24 h at 37˚C, cells were fixed with 4% paraformaldehyde at room temperature for 30 min, then 0.3% Triton X-100 was added (Beijing Solarbio Science & Technology Co., Ltd.) for 15 min at 37˚C. After blocking with 5% BSA for 1.5 h at 37˚C, cells were incubated with the anti-Bax antibody (1:2,000; cat. no. ab32503; Abcam) and anti-Bcl2 antibody (1:2,000; cat. no. ab32124; Abcam) overnight at 4˚C. The cells were then incubated with Alexa Fluor™ 488 goat anti-rabbit IgG (1:5,000; cat. no. A11008; Thermo Fisher Scientific, Inc.) at 37˚C for 1 h in the dark. Following incubation, cells were stained with 1 μg/ml DAPI solution (BD Biosciences) in the dark for 15 min at 37˚C. A fluorescent inverted microscope (magnification, x200; Olympus Corporation) was utilized to capture images of the samples.

Western blot analysis. Total protein was extracted from cells using RIPA lysis buffer (Pierce; Thermo Fisher Scientific, Inc.). Protein concentration was measured using the Pierce BCA Protein Assay kit (Thermo Fisher Scientific, Inc.). Protein samples (50 μg) were separated by SDS-PAGE on an 8% gel and then transferred onto nitrocellulose membranes (Merck KGaA). The separated proteins were subsequently blocked with 5% milk at room temperature for 2 h. The membranes were incubated at 4˚C overnight with the following primary antibodies: Anti-β-actin (1:2,000; cat. no. 66009-1-Ig; ProteinTech Group, Inc.); anti-Bax (1:2,000; cat. no. ab32503; Abcam); anti-Bcl2 (1:2,000; cat. no ab32124; Abcam); and the p53 polyclonal antibody (1:2,000; cat. no. 10442-1-AP; ProteinTech Group, Inc.). Following incubation with primary antibodies, the membranes were incubated with HRP-conjugated goat anti-rabbit IgG (1:5,000; cat. no. ZB2301; OriGene Technologies, Inc.) or goat anti-mouse IgG (1:5,000; cat. no. S0002; Affinity Biosciences, Ltd.) secondary antibodies for 1.5 h at 37˚C. Protein bands were visualized using an ECL kit (cat. no. RPN2232; Cytiva) and a gel imaging system (Bio-Rad Laboratories, Inc.), then analyzed using ImageJ (v1.42q; National Institutes of Health).

Statistical analysis. Statistical analysis was performed using SPSS (version 23.0; IBM Corp.). Each assay was repeated three times. The data are presented as mean ± standard deviation. The difference in CSPG4P12 expression between cancer tissues and adjacent normal tissues was analyzed using paired Student's t-test. The one-way ANOVA test followed by Bonferroni's post hoc correction was utilized to evaluate the result of wound healing assay. The two-tailed Student's t-test was utilized for the analysis of the other experimental data. $P < 0.05$ was considered to indicate a statistically significant difference. The inspection level α was 0.05.
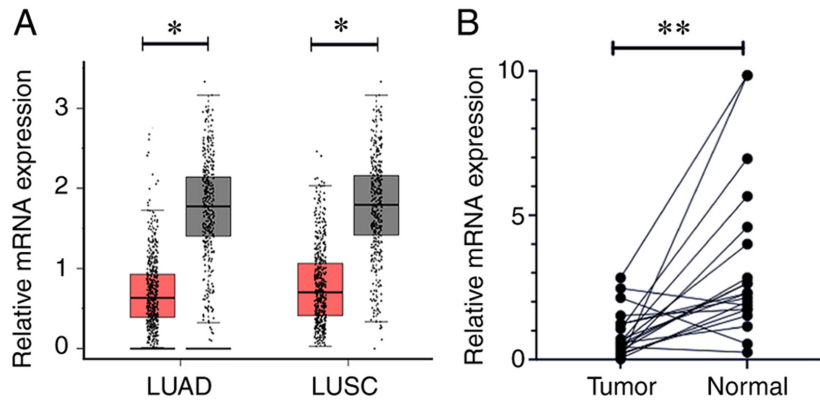
Figure 1. Expression levels of CSPG4P12 in NSCLC and adjacent normal tissues. (A) CSPG4P12 expression in NSCLC tissues as predicted using the gene expression profiling interactive analysis database. The graph represents the following: 483 LUAD tissues (red) and 347 adjacent normal tissues (gray); 486 LUSC tissues (red) and 338 adjacent normal tissues (gray). (B) Reverse transcription-quantitative PCR analysis of CSPG4P12 expression in NSCLC tissues and adjacent normal tissues. *P<0.05 and **P<0.01. CSPG4P12, chondroitin sulfate proteoglycan 4 pseudogene 12; NSCLC, non-small cell lung cancer; LUAD, lung adenocarcinoma. LUSC, lung squamous cell carcinoma.
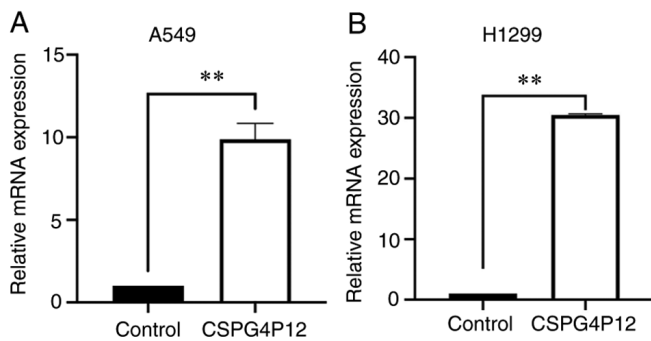

Figure 2. Transfection efficiency as measured using reverse transcription-quantitative PCR analysis. CSPG4P12 expression in (A) A549 and (B) H1299 cells after transfection. **P<0.01. CSPG4P12, chondroitin sulfate proteoglycan 4 pseudogene 12.

Results

Expression of CSPG4P12 is lower in NSCLC tissues compared with that in the adjacent healthy tissues. GEPIA data demonstrated that the expression level of CSPG4P12 in NSCLC tissues was significantly lower compared with that in the adjacent healthy tissues (P<0.05; Fig. 1A). To validate this finding, the expression of CSPG4P12 was detected in 19 pairs of NSCLC tissues and adjacent healthy tissues, which yielded the same outcome (P<0.01; Fig. 1B).

Overexpression of CSPG4P12 inhibits NSCLC cell proliferation. After transfection with CSPG4P12-pUC57, the expression levels of CSPG4P12 were significantly higher compared with those in the control pUC57 plasmid group in both A549 (P<0.01; Fig. 2A) and H1299 cells (P<0.01; Fig. 2B). This suggests that CSPG4P12-pUC57 was successfully transfected into the NSCLC cells tested in the present study. Fig. S1 indicated that transfection of pUC57 plasmid had no effect on cell proliferation. CCK-8 assay results showed that, after CSPG4P12 overexpression for 24, 48 and 72 h, the A549 cell viability was significantly reduced (P<0.01; Fig. 3A). However, it was only at the 48 h timepoint that H1299 cell viability was significantly reduced compared with that in the control pUC57 plasmid group (P<0.01; Fig. 3B). Colony formation assay revealed that the number of cell clones in the CSPG4P12 overexpression group was significantly reduced compared with that in the control plasmid group (P<0.01; Fig. 3C and D).

Overexpression of CSPG4P12 suppresses migration, invasion and adhesion of NSCLC cells. Transwell migration and invasion assays showed that the cell migration and invasion in the CSPG4P12 overexpression group were significantly lower compared with that in the control plasmid group in both cell lines tested (P<0.01; Fig. 4A and B). Wound healing assay showed that, after CSPG4P12 overexpression for 24 and 48 h, wound healing was significantly reduced, which suggested that CSPG4P12 overexpression impaired cell migration (P<0.01; Fig. 4C and D). Cell adhesion experiments indicated that the overexpression of CSPG4P12 significantly decreased A549 cell adhesion 30, 60 and 90 min after transfection with CSPG4P12-pUC57 (P<0.01; Fig. 5).

Overexpression of CSPG4P12 promotes apoptosis by the mitochondria apoptosis pathway. Hoechst33342 fluorescence assay showed that the number of apoptotic cells (dark blue with pyknosis or division) in the control group was markedly lower compared with that in the CSPG4P12 overexpression group (Fig. 6A). In addition, under TEM, some mitochondrial cristaes in the CSPG4P12 overexpression group were either reduced or disappeared, where vacuoles were even formed (Fig. 6B). To explore how CSPG4P12 modulated apoptosis, the expression of apoptosis markers was next measured. Western blot analysis demonstrated that CSPG4P12 overexpression significantly increased the expression of p53 (Fig. 7A and B). Western blotting showed that overexpression of CSPG4P12 markedly decreased the expression of Bcl2; but had no effect on the expression of Bax in A549 cells (Fig. 7A and B). IF assay presented that CSPG4P12 decreased the expression of Bcl2; however, due to the different cell density, we still could not draw the solid conclusion from this assay (Fig. 7C).
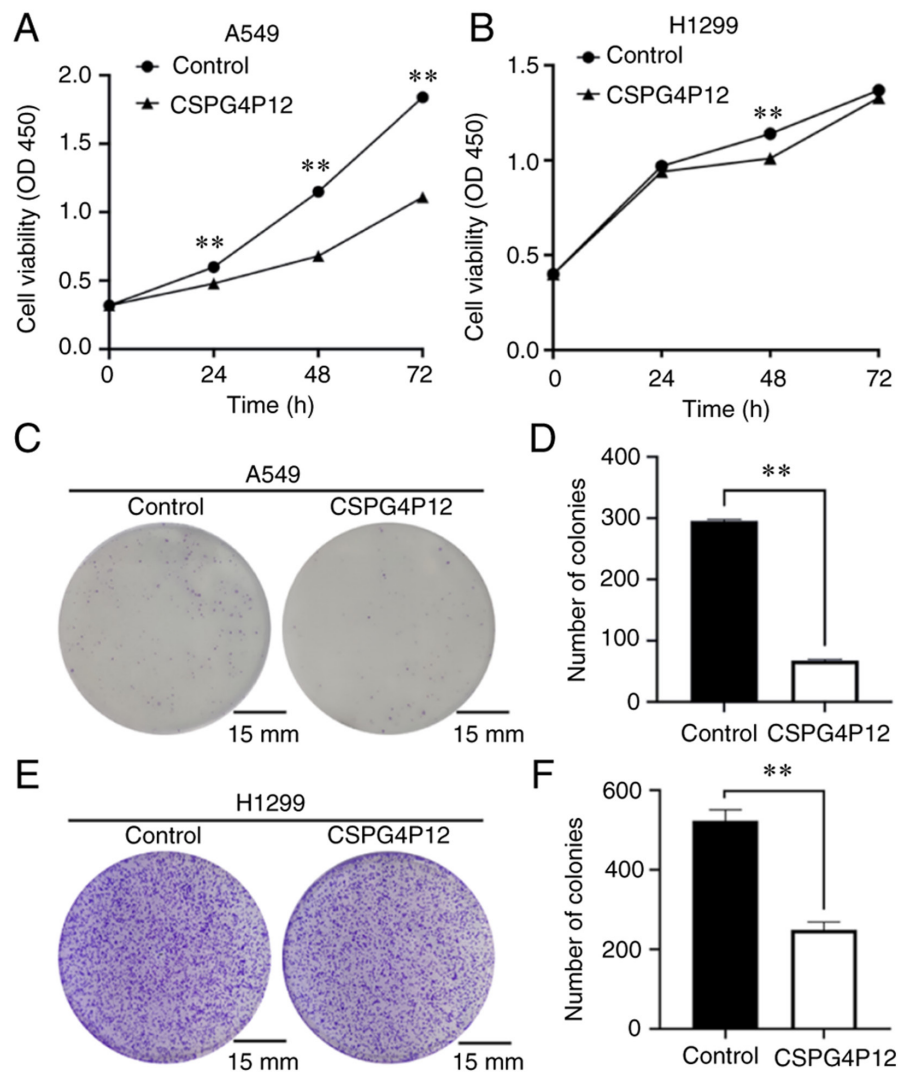
Figure 3. Effects of CSPG4P12 overexpression on the proliferation of non-small cell lung cancer cells. Detection of cell proliferation using Cell Counting Kit-8 assay in (A) A549 cells and (B) H1299 cells. Detection of cell proliferation ability using colony formation assay in (C and D) A549 cells and (E and F) H1299 cells. **P<0.01. CSPG4P12, chondroitin sulfate proteoglycan 4 pseudogene 12; OD_{450}, optical density at 450 nm wavelength.

Discussion

NSCLC remains to be a malignancy with one of the highest rates of morbidity and mortality in the world (7,23). Pseudogene-derived lncRNAs have been reported to be involved in the occurrence and development of NSCLC (12,24). The lncRNA double homeobox A pseudogene 8, which is partially duplicated from myosin light chain kinase (MYLK), is highly expressed in lung adenocarcinoma and can promote cell progression (25). In addition, a previous study revealed that overexpression of MYLK pseudogene 1 can promote the proliferation of NSCLC (26). Therefore, present study focused on CSPG4P12, a lncRNA-derived pseudogene.

CSPG4, the derived gene of CSPG4P12, has been previously found to be overexpressed in triple-negative breast cancer cells (27). Application of the CSPG4 antibody was able to significantly inhibit the proliferation, adhesion and migration of breast cancer cells (27). Furthermore, CSPG4 has been proposed to be a viable immunotherapy target for patients with melanoma (28,29). The present data revealed that overexpressing CSPG4P12 significantly inhibited the cell proliferation,

migration, invasion and adhesion whilst promoting apoptosis in NSCLC cells. These results suggest that CSPG4P12 may be involved in the tumorigenesis and progression of NSCLC.

Apoptosis is fundamental in maintaining the balance between cell division and death. Evasion of apoptosis results in the uncontrolled multiplication of cells that leads to different diseases, including cancer (30). Therefore, apoptosis analysis was performed in the present study to assess the effect of CSPG4P12 on NSCLC. TEM imaging indicated that the overexpression of CSPG4P12 resulted in disappearance of mitochondrial cristae. The damage in the cristae changes the permeability of the mitochondrial membrane, which may induce apoptosis by affecting the expression of mitochondrial proteins, such as Bax and Bcl2 (31). Western blot assay demonstrated that the overexpression of CSPG4P12 facilitated the expression of p53. Previous studies have indicated that p53 induces apoptosis by inhibiting the expression of the anti-apoptotic protein Bcl2 (32,33). By contrast, other studies have previously shown that Bcl-2 and Bax exist as heterodimers where they cooperate with each other to regulate apoptosis (34,35). In the present study, western blotting results supported the hypothesis that the overexpression
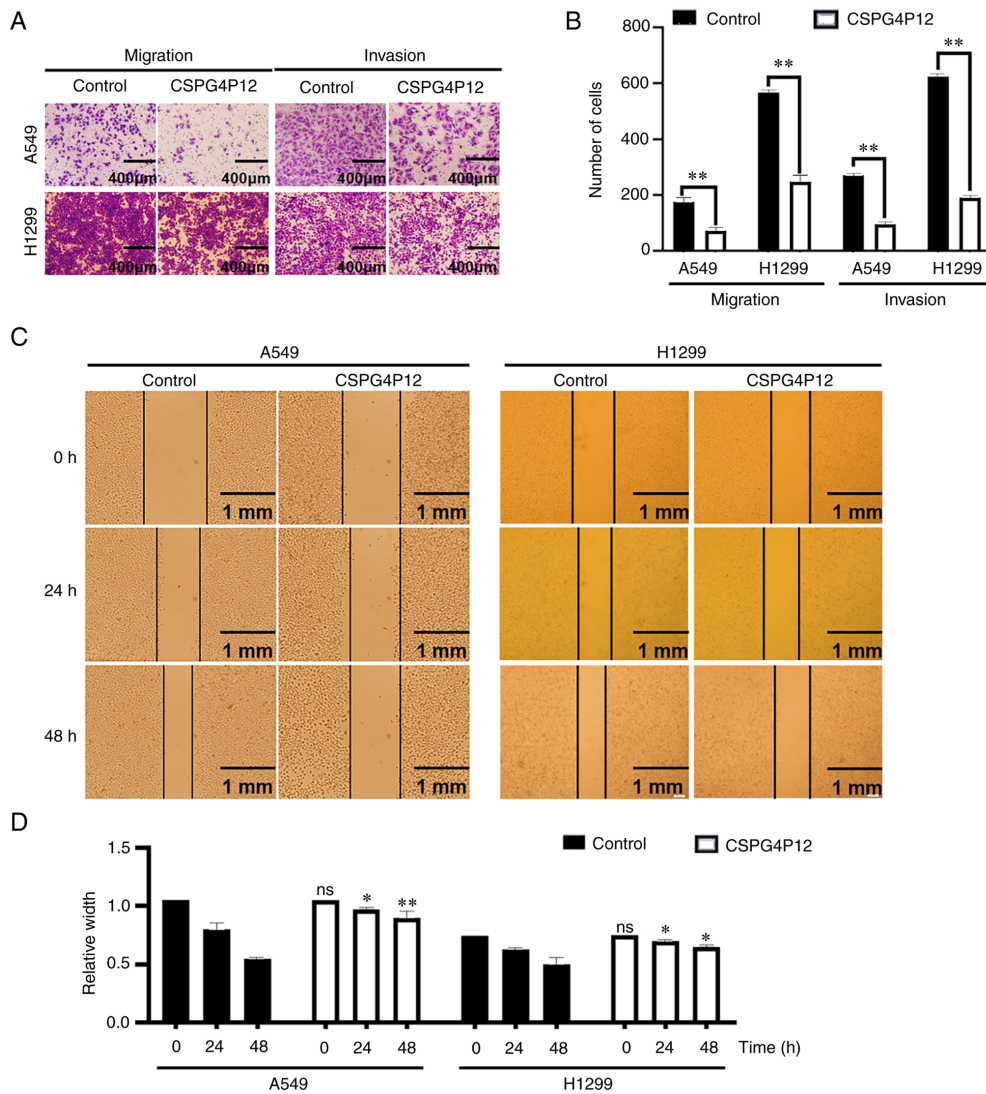
Figure 4. Effects of CSPG4P12 overexpression on migratory and invasive abilities of non-small cell lung cancer cells. Detection of (A) cell migration and invasion using Transwell assay (magnification, x100), (B) the results of which were quantified. (C) Detection and (D) quantification of cell migration using wound healing assay (magnification, x40). *P<0.05 and **P<0.01 vs. control. CSPG4P12, chondroitin sulfate proteoglycan 4 pseudogene 12; ns, not significant.
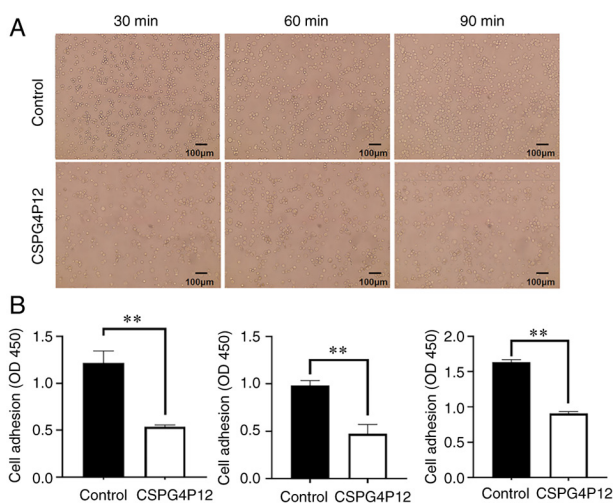

Figure 5. Effects of CSPG4P12 overexpression on the adhesion ability of A549 cells. (A) Images under an inverted light microscope (magnification, x100). (B) Results quantified using Cell Counting Kit-8 assay. **P<0.01. CSPG4P12, chondroitin sulfate proteoglycan 4 pseudogene 12; OD_{450}, optical density measured at 450 nm wavelengths.

of CSPG4P12 promoted apoptosis through the p53/Bcl2/Bax pathway. However, IF assay could not fully demonstrate the effect of CSPG4P12 on the expression of Bcl2 and Bax due to the different cell density. Further experiments still need to be conducted to fully understand this mechanism. Another previous study has demonstrated that CSPG4 immunotoxins combined with a panel of Bcl-2 inhibitors exerted a synergistic effect in mouse xenograft models of glioblastoma, melanoma and breast cancer (36), which indirectly supports the present findings.

There are several limitations that remain associated with the present study. The small sample size of NSCLC tissues hindered the analysis of the association of CSPG4P12 with clinical characteristics of patients with NSCLC. In addition, due to insufficient TEM magnification, the present study did not accurately show the results of mitochondrial damage. However, it was demonstrated that CSPG4P12 functions as a suppressor gene in NSCLC.

In conclusion, CSPG4P12 was found to be downregulated in NSCLC tissues, whilst the overexpression of CSPG4P12 inhibited NSCLC development by activating the p53/Bcl2/Bax axis.
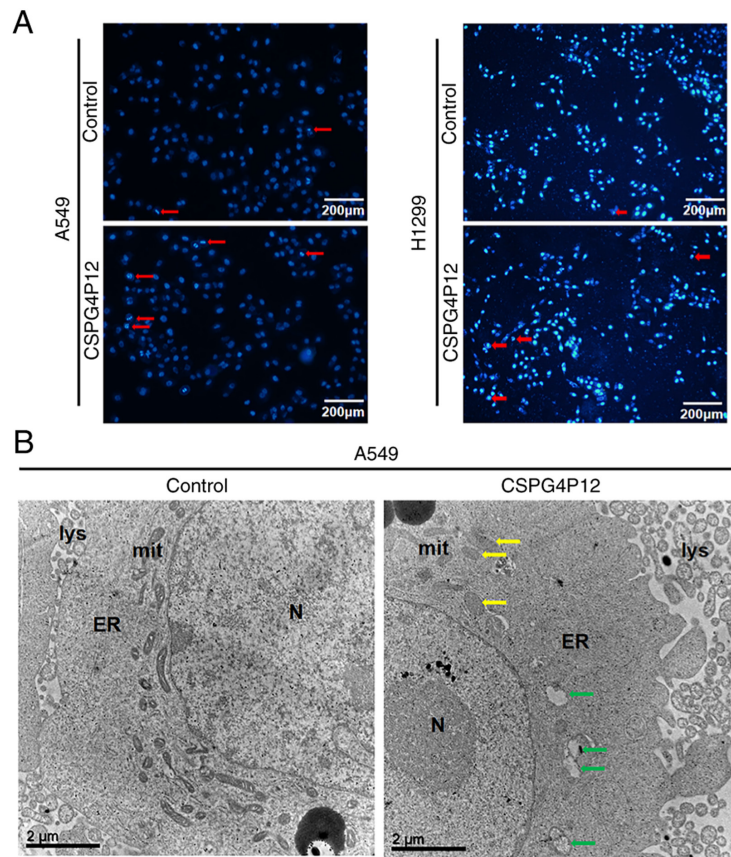
Figure 6. Effects of CSPG4P12 overexpression on the apoptosis of non-small cell lung cancer cells. (A) Fluorescence staining assay (Hoechst 33342; magnification, x100; red arrows indicate apoptotic cells). (B) Transmission electron microscopy (magnification, x10,000; yellow arrows indicate mitochondria with missing cristae; green arrows indicate vacuolated mitochondria). CSPG4P12, chondroitin sulfate proteoglycan 4 pseudogene 12; N, nucleus; ER, endoplasmic reticulum; mit, mitochondria; lys, lysosome.
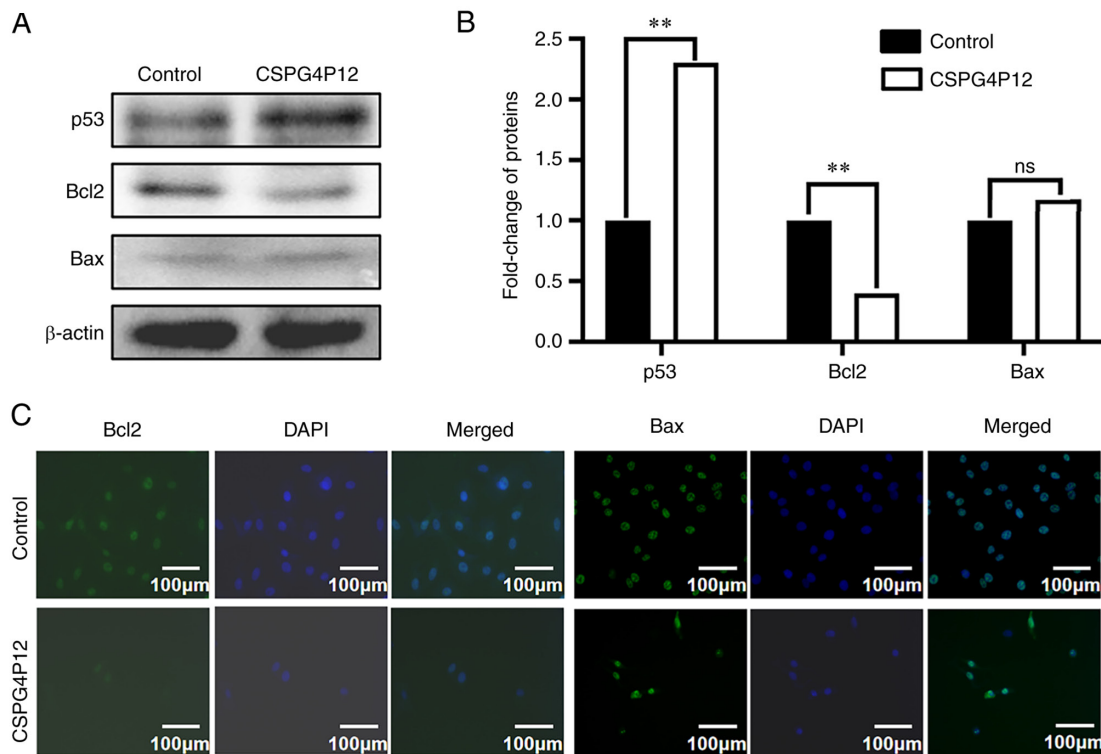

Figure 7. Effects of CSPG4P12 overexpression on apoptosis marker protein expression. (A) Detection of protein expression using western blotting, (B) which was semi-quantified. (C) Detection of Bcl2 and Bax protein expression using immunofluorescence assay (magnification, x200). **$P<0.01$. CSPG4P12, chondroitin sulfate proteoglycan 4 pseudogene 12; ns, not significant.

Availability of data and materials

The datasets used and/or analyzed during the current study are available from the corresponding author on reasonable request.

Authors' contributions

XueZ designed the study. WH, HW, AL and WZ performed the experiments and confirm the authenticity of all the raw data. XuaZ and QT analyzed and interpreted the data. All authors read and approved the final manuscript.

Ethics approval and consent to participate

The present study was approved by the Ethics Committee of North China University of Science and Technology (approval no. 2021036) and all patients or their family members signed informed consent.

Patient consent for publication

Not applicable.

Competing interests

The authors declare that they have no competing interests.

References

1. Siegel RL, Miller KD, Fuchs HE and Jemal A: Cancer Statistics, 2021. CA Cancer J Clin 71: 7-33, 2021.
2. Sung H, Ferlay J, Siegel RL, Laversanne M, Soerjomataram I, Jemal A and Bray F: Global cancer statistics 2020: GLOBOCAN estimates of incidence and mortality worldwide for 36 cancers in 185 countries. CA Cancer J Clin 71: 209-249, 2021.
3. Gadgeel SM, Severson RK, Kau Y, Graff J, Weiss LK and Kalemkerian GP: Impact of race in lung cancer: Analysis of temporal trends from a surveillance, epidemiology and end results database. Chest 120: 55-63, 2001.
4. Norouzi M and Hardy P: Clinical applications of nanomedicines in lung cancer treatment. Acta Biomater 121: 134-142, 2021.
5. El-Hussein A, Manoto SL, Ombinda-Lemboumba S, Alrowaili ZA and Mthunzi-Kufa P: A review of chemotherapy and photodynamic therapy for lung cancer treatment. Anticancer Agents Med Chem 21: 149-161, 2021.
6. Ortega-Franco A, Calvo V, Franco F, Provencio M and Califano R: Integrating immune checkpoint inhibitors and targeted therapies in the treatment of early stage non-small cell lung cancer: A narrative review. Transl Lung Cancer Res 9: 2656-2673, 2020.
7. Duma N, Santana-Davila R and Molina JR: Non-small cell lung cancer: Epidemiology, screening, diagnosis and treatment. Mayo Clin Proc 94: 1623-1640, 2019.
8. Hu X, Yang L and Mo YY: Role of Pseudogenes in tumorigenesis. Cancers (Basel) 10: 45-61, 2018.
9. Sisu C: Pseudogenes as biomarkers and therapeutic targets in human cancers. Methods Mol Biol 2324: 319-337, 2021.
10. Groen JN, Capraro D and Morris KV: The emerging role of pseudogene expressed non-coding RNAs in cellular functions. Int J Biochem Cell Biol 54: 350-355, 2014.
11. Balakirev ES and Ayala FJ: Pseudogenes: Are they 'junk' or functional DNA. Annu Rev Genet 37: 123-151, 2003.
12. Wu C, Song W, Wang Z and Wang B: Functions of lncRNA DUXAP8 in non-small cell lung cancer. Mol Biol Rep 17: 78-92, 2022.
13. Wang XJ, Li XD, Lin FK, Sun HZ, Lin YY, Wang ZL and Wang XP: The lnc-CTSLP8 upregulates CTSL1 as a competitive endogenous RNA and promotes ovarian cancer metastasis. J Exp Clin Cancer Res 40: 151-167, 2021.
14. Hou Z, Wang Y, Xia N, Lv T, Yuan X and Song Y: Pseudogene KRT17P3 drives cisplatin resistance of human NSCLC cells by modulating miR-497-5p/mTOR. Cancer Sci 112: 275-286, 2021.
15. Wiest T, Hyrenbach S, Bambul P, Erker B, Pezzini A, Hausser I, Arnold M, Martin JJ, Engelter S, Lyrer P, *et al*: Genetic analysis of familial connective tissue alterations associated with cervical artery dissections suggests locus heterogeneity. Stroke 37: 1697-1702, 2006.
16. Wang X, Wang Y, Yu L, Sakakura K, Visus C, Schwab JH, Ferrone CR, Favoino E, Koya Y, Campoli MR, *et al*: CSPG4 in cancer: Multiple roles. Curr Mol Med 10: 419-429, 2010.
17. Egan CE, Stefanova D, Ahmed A, Raja VJ, Thiemeyer JW, Chen KJ, Greenberg JA, Zhang TT, He B, Finnerty BM, *et al*: CSPG4 is a potential therapeutic target in anaplastic thyroid cancer. Thyroid 31: 1481-1493, 2021.
18. Yang J, Liao Q, Price M, Moriarity B, Wolf N, Felices M, Miller JS, Geller MA, Bendzick L, Hopps R, *et al*: Chondroitin sulfate proteoglycan 4, a targetable oncoantigen that promotes ovarian cancer growth, invasion, cisplatin resistance and spheroid formation. Transl Oncol 16: 101318, 2022.
19. Poliseno L, Salmena L, Zhang J, Carver B, Haveman WJ and Pandolfi PP: A coding-independent function of gene and pseudogene mRNAs regulates tumour biology. Nature 465: 1033-1038, 2010.
20. Liu J, Liu ZX, Wu QN, Lu YX, Wong CW, Miao L, Wang Y, Wang ZX, Jin Y, He MM, *et al*: Long noncoding RNA AGPG regulates PFKFB3-mediated tumor glycolytic reprogramming. Nat Commun 11: 1507-1523, 2020.
21. Tang ZF, Kang BX, Li CW, Chen TX and Zhang ZM: GEPIA2: An enhanced web server for large-scale expression profiling and interactive analysis. Nucleic Acids Res 47: W556-W560, 2019.
22. Livak KJ and Schmittgen TD: Analysis of relative gene expression data using real-time quantitative PCR and the 2(-Delta Delta C(T)) method. Methods 25: 402-408, 2001.
23. Parkin DM: Global cancer statistics in the year 2000. Lancet Oncol 2: 533-543, 2001.
24. Lou W, Ding B and Fu P: Pseudogene-derived lncRNAs and their miRNA sponging mechanism in human cancer. Front Cell Dev Biol 8: 85-87, 2020.
25. Yin D, Hua L, Wang J, Liu Y and Li X: Long non-coding RNA DUXAP8 facilitates cell viability, migration and glycolysis in non-small-cell lung cancer via regulating HK2 and LDHA by inhibition of miR-409-3p. Onco Targets Ther 13: 7111-7123, 2020.
26. Han YJ, Ma SF, Yourek G, Park YD and Garcia JG: A transcribed pseudogene of MYLK promotes cell proliferation. FASEB J 25: 2305-2312, 2011.
27. Wang XH, Osada T, Wang YY, Yu L, Sakakura K, Katayama A, McCarthy JB, Brufsky A, Chivukula M, Khoury T, *et al*: CSPG4 protein as a new target for the antibody-based immunotherapy of triple-negative breast cancer. J Natl Cancer Inst 102: 1496-1512, 2010.
28. Mittelman A, Chen ZJ, Kageshita T, Yang H, Yamada P, Baskind P, Goldbery N, Puccio C, Ahmed T, *et al*: Active specific immunotherapy in patients with melanoma. A clinical trial with mouse antiidiotypic monoclonal antibodies elicited with syngeneic anti-high-molecular-weight-melanoma-associated antigen monoclonal antibodies. J Clin Invest 86: 2136-2144, 1990.
29. Mittelman A, Chen ZJ, Yang H, Wong GY and Ferrone S: Human high molecular weight melanoma-associated antigen (HMW-MAA) mimicry by mouse anti-idiotypic monoclonal antibody MK2-23: Induction of humoral anti-HMW-MAA immunity and prolongation of survival in patients with stage IV melanoma. Proc Natl Acad Sci USA 89: 466-470, 1992.
30. Jan R and Chaudhry GE: Understanding apoptosis and apoptotic pathways targeted cancer therapeutics. Adv Pharm Bull 9: 205-218, 2019.

31. Precht TA, Phelps RA, Linseman DA, Butts BD, Le SS, Laessig TA, Bouchard RJ and Heidenreich KA: The permeability transition pore triggers Bax translocation to mitochondria during neuronal apoptosis. Cell Death Differ 12: 255-265, 2005.
32. Dashzeveg N and Yoshida K: Cell death decision by p53 via control of the mitochondrial membrane. Cancer Lett 367: 108-112, 2015.
33. Bai HL, Kang CM, Sun ZQ, Li XH, Dai XY, Huang RY, Zhao JJ, Bei YR, Huang XZ, Lu ZF, et al: TTDA inhibited apoptosis by regulating the p53-Bax/Bcl2 axis in glioma. Exp Neurol 331: 113380-113398, 2020.
34. Campbell KJ and Tait SWG: Targeting BCL-2 regulated apoptosis in cancer. Open Biol 8: 203-219, 2018.
35. Zhang J, Xie Y, Fan Q and Wang C: Effects of karanjin on dimethylhydrazine induced colon carcinoma and aberrant crypt foci are facilitated by alteration of the p53/Bcl2/BAX pathway for apoptosis. Biotech Histochem 96: 202-212, 2021.
36. Yu X, Dobrikov M, Keir ST, Gromeier M, Pastan IH, Reisfeld R, Bigner DD and Chandramohan V: Synergistic antitumor effects of 9.2.27-PE38KDEL and ABT-737 in primary and metastatic brain tumors. PLoS One 14: 38-54, 2019.